Oriented Immobilization of Antibodies for Immunosensing

ARTICLE *in* LANGMUIR · JUNE 1998

Impact Factor: 4.46 · DOI: 10.1021/la971412x

2 AUTHORS:

Inger Vikholm-Lundin
University of Tampere
92 PUBLICATIONS **1,142** CITATIONS
SEE PROFILE

Martin Albers
BioNavis Ltd
61 PUBLICATIONS **613** CITATIONS
SEE PROFILE

Oriented Immobilization of Antibodies for Immunosensing

I. Vikholm* and W. M. Albers

Technical Research Centre of Finland, Chemical Technology, P.O. Box 14021, 33101 Tampere, Finland

Received December 23, 1997

The covalent coupling of antibody fragments to linkers embedded in a monolayer matrix of phosphatidylcholine and cholesterol was examined at the air−water interface by the means of a quartz crystal microbalance, QCM. Two linkers that bind the free thiols of the Fab′ fragment were investigated. The nonspecific binding of bovine serum albumin and the specific binding of antigen were also monitored with the QCM. Standardized radioimmunoassay was used to confirm the immunoreaction and determine binding parameters. The monolayer formation of the linker lipids in the ternary system of phosphatidylcholine and cholesterol was, moreover, demonstrated by film balance studies. The results demonstrate that the covalent coupling of Fab′ fragments to linking groups embedded in a phospholipid monolayer matrix is a promising approach to achieve a defined immobilization of antibodies at the sensor surface with high antigen binding effeciency.

Introduction

Immunoassays are commonly used to measure the concentration of a variety of hormones, allergens, viruses, and bacteria in clinical laboratory tests. Such tests are of great importance in the diagnosis of cancer, HIV, BSE, and others. Presently, much effort is put in the development of immunoassays, which allow monitoring of the antigen−antibody binding directly and which do not require the use of labeled species.[1−11] The biomolecules have to be attached to a transducer surface with optimal preservation of their binding activity and specificity. Methods widely used are physical adsorption,[1,2] covalent coupling,[3−5] cross-linking, or entrapment in a gel network. Neither of these methods can guarantee a proper orientation of the biomolecules, and the antibodies may thus be inhibited from binding due to shielding of the antigen-binding domains. Furthermore, there are problems concerning the reproducibility and homogeneity of the layers. Protein A or protein G has been commonly used to orient antibodies for immunoassay,[2,3,6] and the specific bindings of streptavidin to biotin-functionalized monolayers have been used to obtain layers of orientated antibodies.[7] Recently, the Langmuir−Blodgett (LB) technique has been employed to more effectively control the orientation and surface density of antibodies.[7−12] Antibodies have been spread directly onto the air−water interface or adsorbed onto preformed monolayers.[8,9] To obtain site-directed immobilization, it is, however, necessary to make the antibodies amphiphilic.[10−12] The antigen-binding capability of lipid-tagged single-chain antibodies incorporated into various lipid monolayers has been demonstrated with surface plasmon resonance.[11,12]

The present research is related to the attachment of biomolecules to liposomes via linker lipids.[13] This subject has attracted a great deal of interest because of the potential use of liposomes as targeted drug delivery systems.[14,15] It has only recently been proposed that the attachment of Fab′ fragments to linker lipids is a promising way of preparing high-quality films for diagnostic applications.[16−18] Reduction of the disulfide bridges in the hinge region of an $F(ab')_2$ fragment yields well-accessible and reactive thiol groups, which are located opposite the antibody-binding domain. Egger et al. has coupled Fab′ fragments covalently to small unilamellar vesicles and allowed these to fuse at the air−water interface to form monomolecular films of Fab′ fragments.[17]

The quartz crystal microbalance (QCM) is based on changes in the resonant frequency of a piezoelectric crystal that take place upon adsorption of material on the surface of the gold electrodes.[19,20] The QCM has been used for detection of gases,[20,21] hydration of lipid layers,[22] and determination of specific interactions between surface-bound receptors and analytes.[23−25] The QCM can also be

* To whom the correspondence should be addressed. Telephone: +358 3 3163 363. Fax: +358 3 3163 319. E-mail: inger.vikholm@vtt.fi.

(1) Sandwick, R.; Schray, K. J. *J. Colloid Interface Sci.* **1988**, *121*, 1.
(2) Caruso, F.; Rodda, E.; Furlong, D. N. *J. Colloid Interface Sci.* **1996**, *178*, 104.
(3) Tamiya, E.; Watanabe, N.; Matsuoka, H.; Karube, I. *Biosensors* **1987/88**, *3*, 139.
(4) Feng, C.-D.; Ming, Y.-D.; Hesketh, P. J.; Gendel, S. M.; Stetter, J. R. *Sens. Actuators* **1996**, *B35*, 431.
(5) Williams, R. A.; Blanch, H. W. *Biosens. Bioelectron.* **1994**, *9*, 159.
(6) Lekkala, J. O.; Sadowski, J. W. *Chem. Sens. Technol.* **1994**, *5*, 199.
(7) Häussling, L.; Ringsdorf, H.; Schmitt F. J.; Knoll, W. *Langmuir* **1991**, *7*, 1837.
(8) Ahluwalia, A. *Thin Solid Films* **1992**, *210/211*, 726.
(9) Barraud, A.; Perrot, H.; Billard, V.; Martelet, C.; Therasse, J. *Biosens. Bioelectron.* **1993**, *8*, 39.
(10) Ahluwalia, A.; Carra, M.; De Rossi, D.; Ristori, C.; Tundo, P.; Bomben, A. *Thin Solid Films* **1994**, *247*, 244.
(11) Vikholm, I.; Peltonen, J. *Thin Solid Films* **1996**, *284−285*, 924.
(12) Vikholm, I.; Györvary, E.; Peltonen, J. *Langmuir* **1996**, *12*, 3276.
(13) Heath, T. D. *Methods Enzymol.* **1987**, *149*, 111.
(14) Rongen, H. A. H.; Bult, A.; Bennekom, W. P. *J. Immunol. Methods* **1997**, *204*, 105.
(15) Heat, T. D.; Fraley, R. T.; Papahadjopoulos, D. *Science* **1980**, *210*, 539.
(16) Jimbo, Y.; Saito, M. *J. Mol. electron.* **1988**, *4*, 111.
(17) Egger, M.; Heyn, S. P.; Gaub, H. E. *BBA* **1992**, *1104*, 45.
(18) Lu, B.; Xie, J.; Lu, C.; Wu, C.; Wei, Y. *Anal. Chem.* **1995**, *67*, 83.
(19) Sauerbrey, G. *Z. Phys.* **1959**, *155*, 206.
(20) Meccea, V. M. *Sens. Actuators A* **1994**, *40*, 1.
(21) Schmautz, A. *Sens. Actuators B* **1992**, *6*, 38.
(22) Wakamatsu, K.; Hosoda, K.; Mitomo, H.; Ohya, M.; Okahata, Y.; Yasunaga, K. *Anal. Chem.* **1995**, *67*, 3336.
(23) Suri, C. R.; Raje, M.; Mishra, G. C. *Biosensens. Bioelectron.* **1994**, *9*, 535.
(24) Ngeh-Ngwainbi, J.; Suleiman, A. A.; Guilbault, G. G. *Biosens. Bioelectron.* **1990**, *5*, 13−26.
(25) Geddes, N. J.; Paschinger, E. M.; Furlong, D. N.; Caruso, F.; Hoffmann, C. L.; Rabolt, J. F. *Thin Solid Films* **1995**, *260*, 192.

S0743-7463(97)01412-1 CCC: $15.00
Published on Web 06/16/1998

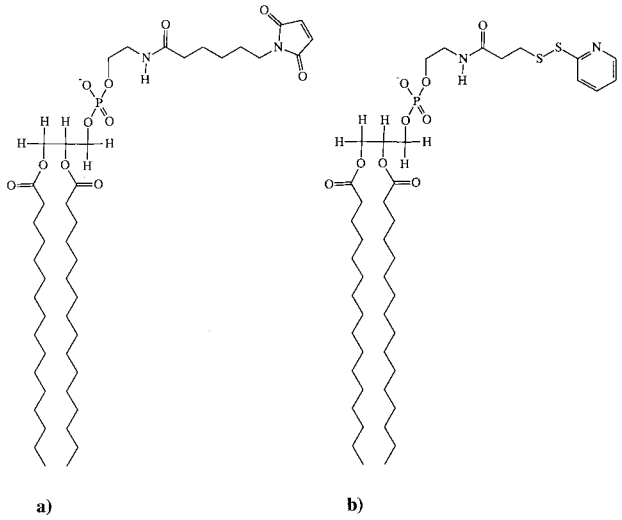

Figure 1. Structure of the linker molecules for covalent coupling of Fab′ fragments: (a) DPPE-EMCS; (b) DPPE-SPDP.

applied to studies of DNA hybridization,[26] drug release[27] and electrodeposition.[28] Measurements have till recently been performed predominantly in air, but it is also possible to observe the binding reactions of proteins in situ in aqueous solution.[29−32] The quenching of the QCM oscillation in liquids can be prevented by immersion of only one side of the quartz crystal in liquid and using frequency-dependent admittance analysis.[31,33,34]

Our approach has been to embed lipids with terminal linker groups into a monolayer of phosphatidylcholine at the air−water interface and covalently attach Fab′ fragments to these layers.[34] In this paper, the monolayer formation of two linker lipids in ternary mixed systems of phosphatidylcholine and cholesterol will first be described. Second, the coupling of Fab′ fragments and the subsequent binding of human immunoglobulin G to the monolayers will be quantitatively assessed by in situ QCM measurements. Finally, standardized radioimmunoassay was performed to assess the immunological binding parameters.

Experimental Section

Synthesis of Linker Lipids. The linker lipid *N*-(ϵ-maleimidocaproyl)-dipalmitoylphosphatidylethanolamine (DPPE-EMCS, , Figure 1a) was prepared by the reaction of *N*-(ϵ-maleimidocaproyl)succinimide (EMCS, Fluka, >98%) with dipalmitoyl-*sn*-glycero-phosphatidylethanolamine (DPPE, Fluka, >99%) using triethylamine (Baker, >98%) as a homogeneous catalyst.[13] *N*-[3-(2-pyridyldithio)propionyl]dipalmitoylphosphatidylethanolamine (DPPE-SPDP, Figure 1b) was prepared by a similar reaction of dipalmitoyl-*sn*-glycero-phosphatidylethanolamine with *N*-succinimidyl 3-(2-pyridyldithio)propionate. Both linker lipids were purified by chromatography on silica gel (Si 60) using mixtures of chloroform with increasing amounts of methanol.[13] The final products were analyzed with 600 MHz ^{1}H NMR.

Monolayer Formation. The host matrix lipids 1,2-dipalmitoyl-*sn*-glycero-3-phosphatidylcholine (DPPC, Sigma, >99%) and cholesterol (CHOL, KSV Chemicals, 99.8%) were mixed in various ratios with 10 mol % linker lipid and spread onto an aqueous subphase of 10 mM HEPES, 150 mM NaCl at pH = 6.8 for DPPE-EMCS and pH = 7.2 for DPPE-SPDP. The monolayers were prepared in a homemade Teflon trough with dimensions of 50 × 200 × 10 mm^3 using a commercial LB instrument (KSV 2000 LB, Finland).

Model Antibodies. The model antibody was polyclonal goat anti-human F(ab′)$_2$ (Jackson ImmunoResearch, chromatically purified) with minimized cross-reaction to bovine, horse, and mouse serum proteins. The antigen was chromatically purified human IgG (Jackson ImmunoResearch). F(ab′)$_2$ was split into Fab′ fragments with dithiothreitol (DTT, Merck) prior to use as follows:[35] F(ab′)$_2$ with a concentration of 1.2−1.3 mg/mL (100 μL) was mixed with 50 μL of HEPES/EDTA buffer (150 mM NaCl, 10 mM HEPES, 5 mM EDTA, pH = 6.0) and 10 μL of a 0.1 M DTT solution in HEPES/EDTA buffer in a microdialysis tube. The dialysis tube was immersed in 250 mL of argon-purged HEPES/EDTA buffer and dialyzed for about 18 h at room temperature under argon. The Fab′ fragment was maintained under argon and used within a few days for coupling.

Quartz Crystal Microbalance. The resonators used in this study were 10 MHz AT-cut quartz crystals with gold electrodes (Universal Sensors, Inc., New Orleans). The quartz plate diameter was 14 mm, and the gold electrode diameter was 8 mm. The edges of the resonators were covered with a ring of silicone rubber (Dow Corning Corporation). The silicone rubber prevented corrosion of the wires and degradation of the electrical contacts when submersed in solution. Furthermore, the silicone rubber improved the stability of the device 3-fold to a noise level of 0.45 Hz in one-sided contact with water. The precision of the instrument was very high. Surface mass densities of the deposited film could be determined with an error less than 1 ng/cm^2 using Sauerbreys' equation:[19]

$$\delta F = -2\frac{F^2}{\sqrt{\mu_q \rho_q}}\frac{\delta m}{A} \qquad (1)$$

where F is the fundamental oscillation frequency and δF is the observed shift in the frequency of the coated crystal, μ_q is the shear modulus of AT-cut quartz (2.947×10^{10} kg m^{-1} s^{-2}), ρ_q is the density of quartz (2648 kg m^{-3}), and A is the area of the gold electrode. In aqueous solution this is, however, an approximation, as the viscosity and elasticity effects of the layer and, moreover, embedded water also may play an important role.

A Hewlett-Packard 4195A spectrum/network analyzer connected to a computer was used to gather the near resonance admittance phase spectra with a sample time of 1 min. The system automatically traced the approximate resonant frequency and adjusted a frequency range of 200 Hz around it. Hereafter the spectrum was rapidly sampled 10 times. A mean value of the samples was taken, and a linear regression estimate for the resonant frequency was calculated. The gold electrode was generally cleaned with chromosulfuric acid, rinsed with water, and air-dried before measurement. With this procedure the same crystal could be used a large number of times, although a gradual increase of the noise level was observed.

In Situ Measurements with the QCM. The monolayer containing the linker lipid was compressed to the surface pressure 40 mN/m, and one side of the QCM was lowered to make horizontal contact with the monolayer (Figure 2). HEPES/EDTA was flushed through the Teflon cell placed beneath the monolayer for about 3 min by the means of a peristaltic pump. This allowed a homogeneous and reproducible mixing of the solution. The phase angle shift was recorded until a steady value was obtained. An initial increase in frequency was noticed due to disturbances caused by the peristaltic pump. The antibody stock solution was hereafter introduced beneath the monolayer, followed by 100 μg/mL of BSA to block unspecific binding sites and by various concentrations of human IgG. The frequency changes due to the binding of protein were monitored as a function of time for 0.5

(26) Caruso, F.; Rodda, E.; Furlonf, D. N.; Niikura, K.; Okahata, Y. *Anal. Chem.* **1997**, *69*, 2043.
(27) Hepel, M.; Mahdavi, F. *Microchem. J.* **1997**, *56*, 54.
(28) Burgess, J. D.; Hawkridge, F. M. *Langmuir* **1997**, *13*, 3781.
(29) Köβlinger, C.; Uttenthaler, E.; Dorst, S.; Aberl, F.; Wolf, H.; Brink, G.; Stanglmaier, A.; Sackmann, E. *Sens. Actuators B* **1995**, *24−25*, 107.
(30) Kösslinger, C.; Dorst, S.; Aberl, F.; Wolf, H.; Koch, S.; Woias, P. *Biosens. Bioelectron.* **1992**, *7*, 397.
(31) Rickert, J.; Brecht, A.; Göpel, W. *Anal. Chem.* **1997**, *69*, 1441.
(32) Steegborn, C.; Skàdal, P. *Biosens. Bioelectron.* **1997,** *12*, 19.
(33) Välimäki, H.; Lekkala, J.; Helle, H. *Sens. Actuators* **1997**, *A60*, 80.
(34) Vikholm, I.; Albers, M.; Välimäki, H. *Thin Solid Films*, accepted.
(35) Ishikawa, E. *J. Immunoassay* **1983**, *4*, 209.

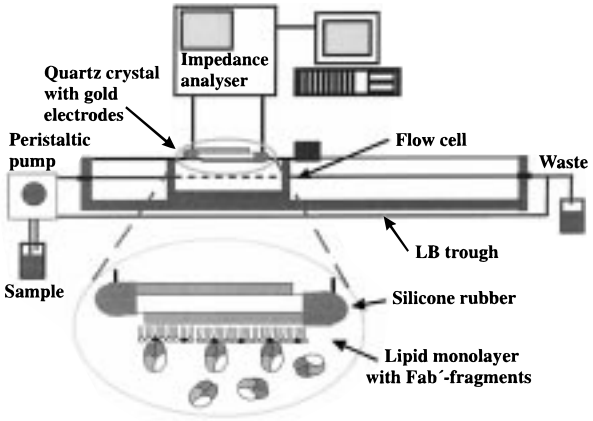

Figure 2. Schematic illustration of the QCM setup. Fab′ solution was pumped into a Teflon cell placed beneath the monolayer, and the shift in resonant frequency was recorded.

h. At the end of each measuring series the QCM was raised from the air−water interface, rinsed with water, and air-dried. These ΔF values were compared with those obtained in liquid.

Radioimmunoassay. Silicon substrates with the dimensions 6×9 mm^2 were peroxide-treated to generate a maximum amount of silanol groups on the surface. The slides were coated with octadecyltrichlorosilane (ODTCS, Aldrich 95%) from toluene solutions, rinsed with toluene, and air-dried. Linker lipids embedded in a host monolayer matrix of DPPC with or without CHOL were then horizontally transferred onto these supports, as earlier described.[34] Anti-human Fab′ (50 μg/mL of Fab′ HEPES buffer, pH = 6.8) was subsequently bound to the layers in 2 h at room temperature using a thin film reaction chamber with a volume of 30 mL. The slides were hereafter transferred to PBS buffer (0.15 M NaCl, 10 mM KH_2PO_4, pH = 7.5) containing 0.5 g/L of BSA (bovine serum albumin, Sigma RIA grade) and left in this solution at 4 °C for 18 h. The series of silicon slides were then incubated in a microtiter plate with increasing standardized amounts of human IgG in the presence of a constant amount of ^{125}I-labeled human IgG and BSA (3.3−5.0 g/L). The amount of Fab′ immobilized was also assessed by a standardized radiotracer method, using ^{125}I-labeled Fab′. The radiolabeled Fab′ had gone simultaneously through all other process steps (dilution and F(ab′)$_2$ splitting) in the same way as the unlabeled Fab′, to ensure that the label was similar in chemical reactivity.

Results and Discussion

Monolayer Formation. DPPC displayed a surface pressure−area curve characteristic for saturated phospholipids transforming from the liquid expanded to the condensed phase below 5 mN/m (Figure 3a, inset). The phase transition, however, became less pronounced when 10 mol % of the linker lipids was included in the layer. The linking groups were oriented in a different way in the DPPC monolayer matrix. If an ideal mixing is assumed, the molecular surface area of the linker lipids could be estimated.[36] The mean molecular area of DPPE-EMCS at the surface pressure 40 mN m^{-1} was 102.5 Å^2, whereas that of DPPE-SPDP was twice this value, 210.5 Å^2. The mean molecular area of cholesterol was 35.6 Å^2/molecule (Figure 3a), in agreement with the data reported by Takano et al.[37] Cholesterol had a condensing effect on the monolayers (Figures 3 and 4a). The extent of condensation (C) can be calculated according to the ratio:[38] $C = (A - A_{exp})/A$, where A is the molecular surface area calculated from the surface area of the pure components with ideal mixing[36] and A_{exp} is the molecular surface area

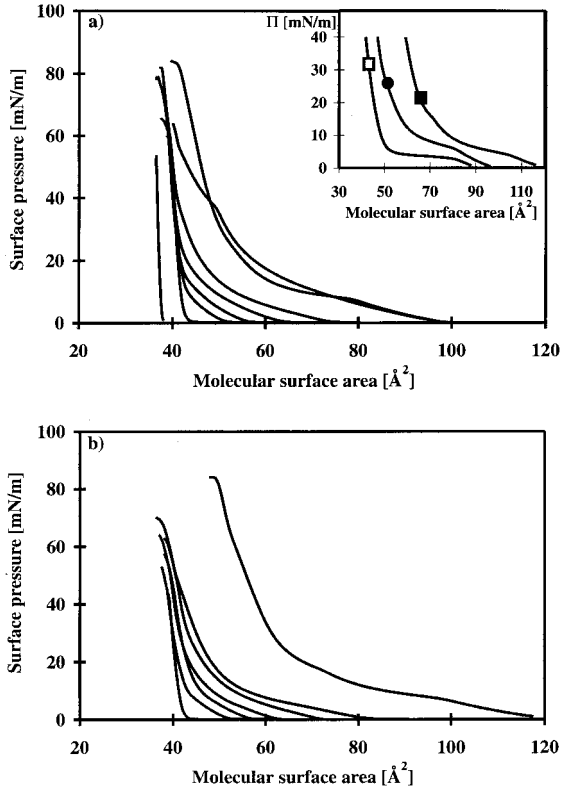

Figure 3. Surface pressure−area isotherms of ternary mixed system of DPPC, linker molecules (10 mol %), and cholesterol (0, 10, 20, 30, 40, 50, 70, and 100 mol % from right to left): (a) DPPE-EMCS; (b) DPPE-SPDP. The inset shows the isotherms of DPPC (□), DPPE-EMCS (●) and DPPE-SPDP (■).

obtained from the experimental isotherm. Maximal condensation occurred at about 15 mol % CHOL (Figure 4a, inset). The condensing effect of CHOL on DPPE-SPDP is higher than that on DPPE-EMCS. At about 30 mol % CHOL the mean molecular areas of the molecules became equal (Figure 4a). DPPC/DPPE-EMCS exhibits a phase transition around 35 mN/m if only 10 mol % cholesterol was included in the layer (Figure 3a). DPPE-EMCS is probably squeezed out of the layer at this surface pressure as the collapse pressure of the pure linker occurs around 45 mN/m (data not shown).

The stability of the DPPC/linker/CHOL monolayers was assessed by compressing the monolayers to a surface pressure of 40 mN/m and by measuring the ratio of molecular area $A(t)$ at time t and that at zero. The shape of $R_s = A(t)/A(0)$ against time was concave, which excludes a monolayer collapse (data not shown).[39] The concavity of the relaxation curve was merely due to a reorganization of molecules and a partial dissolution into the subphase. The relaxation was minor after 40 min, and Figure 4 shows that the stability of the monolayers depends on the linker molecule. The relaxation decreased in the order DPPC/DPPE-SPDP < DPPC/DPPE-EMCS < DPPC. Cholesterol has, moreover, a stabilizing effect on the monolayers. The stabilizing effect of cholesterol has also been demonstrated with vesicles,[40] black lipid membranes,[41,42] and DPPC monolayers.[43,44]

(36) Vikholm, I.; Helle, H. *Thin Solid Films* **1989,** *178*, 197.
(37) Takano, E.; Ishida, Y.; Iwahashi, M.; Araki, T.; Iriyama, K. *Langmuir* **1997**, *13*, 5782.
(38) Grönberg, L.; Slotte, J. P. *Biochemistry* **1990**, *29*, 3173.
(39) Binks, B. P. *Adv. Colloid Interface Sci.* **1991**, *34*, 343.
(40) Needham, D.; Nunn, R. S. *Biophys. J.* **1990**, *58*, 997.
(41) Snejdàrkovà, M.; Rehàk, M.; Otto, M. *Biosens.Bioelectron.* **1997,** *12*, 145.
(42) Yamauchi, H.; Takao, Y.; Abe, M.; Ogino, K. *Langmuir* **1993,** *9*, 300.
(43) Weis, R.; McConnel, H. M. *J. Phys. Chem.* **1985**, *89*, 4453.

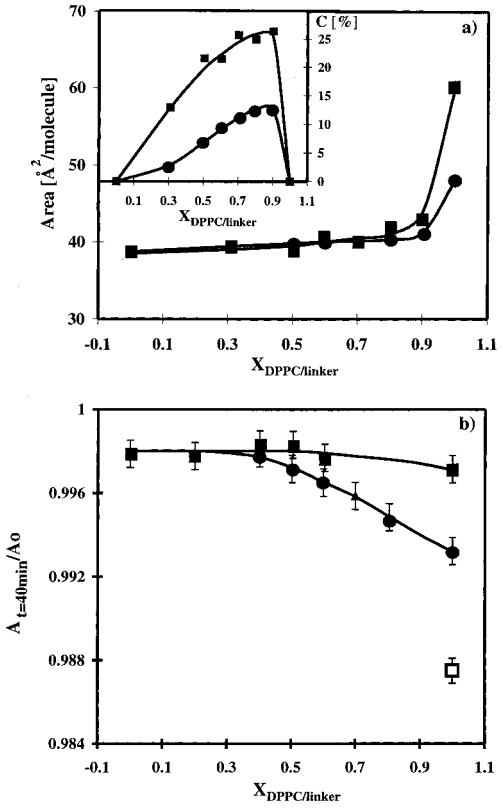

Figure 4. (a) Mean molecular area of the ternary system of DPPC/linker/CHOL at the surface pressure 40 mN/m versus DPPC/linker mole fraction. The inset shows the cholesterol-induced condensation. (b) Stability of the DPPC/linker/CHOL monolayers at the air−water interface at 40 mN/m expressed as the ratio of the molecular surface area at $t = 40$ min and time zero versus DPPC/linker mole fraction: DPPE-SPDP, (■), DPPE-EMCS (●), and DPPC (□).

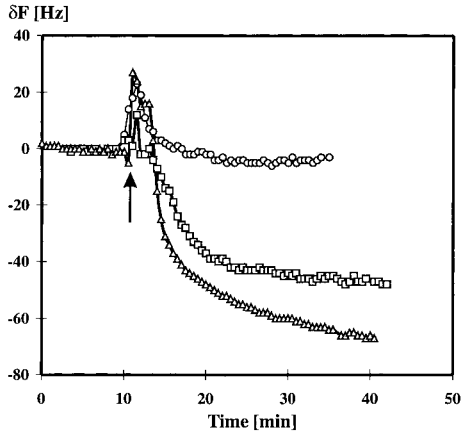

Figure 5. Change in resonant frequency versus time upon binding of 25 μg/mL of $F(ab')_2$ fragments (○), and 10 μg/mL (□) and 25 μg/mL (△) of Fab′ fragments to a monolayer of DPPC/DPPE-EMCS (9/1). The arrow indicates the time at which antibody fragments were pumped into the cell.

Dependence on Fab′ Fragment Concentration. The QCM frequency changes, during the immobilization of antibody fragments onto a monolayer of DPPC/DPPE-EMCS from 10 and 25 μg/mL Fab′ fragment solutions and a 25 μg/mL $F(ab')_2$ solution, are shown in Figure 5. No change in frequency was observed when $F(ab')_2$ fragments were pumped into the cell beneath the monolayer. This

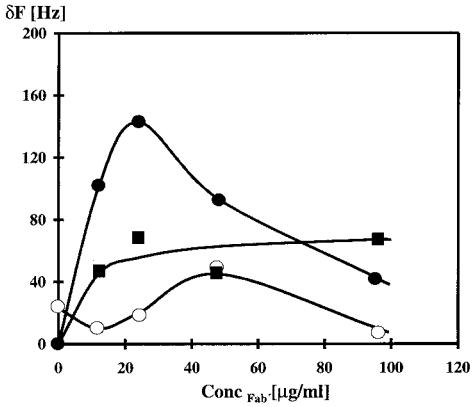

Figure 6. Total change in frequency upon binding of Fab′ fragments (■), 0.1 mg/mL of BSA (○), and 0.1 mg/mL of human IgG (●) to a monolayer of DPPC/DPPE-EMCS (9/1) versus Fab′ fragment concentration.

is opposite to what has been reported by Ben-Dov et al.[45] They coupled $F(ab')_2$ anti-mouse IgG to maleimide linkers in a self-assembled monolayer and obtained a decrease in resonant frequency of 89 Hz after drying the layer. However, there are no free thiol groups in the $F(ab')_2$ fragment available for reaction with the linker group and any binding should thus be due to unspecific adsorption. In our case, as illustrated in Figure 5, we could not observe any binding to the layer, unless the $F(ab')_2$ had been split into Fab′ fragments with dithiothreitol. Figure 5 shows that the Fab′ fragments gave rise to a decrease in frequency with time, which reflects the covalent attachment of fragments to the layer. Binding equilibrium was achieved within about 15−30 min. It should be noted that the initial increase in frequency was due to disturbances from pumping of the buffer. The binding was dependent on the Fab′ fragment concentration. A saturation value of 60 Hz was reached at a Fab′ fragment concentration of about 25 μg/mL (Figure 6).

The subsequent unspecific binding of BSA as a function of Fab′ fragment concentration is also shown in Figure 6. A frequency decrease of 25 Hz was observed if no Fab′ fragments were attached to the layer. The amount of unspecific adsorption, however, decreased if Fab′ fragments were bound to the layer from lower concentrations. The amount of Fab′ bound to the lipid layer increased with Fab′ concentration up to 50 μg/mL, displaying a maximum frequency change of 50 Hz. We also noticed that the nonspecific binding of BSA was very low for the highest Fab′ concentrations used.

When the antigen, human IgG, was introduced into the cell with a gradual increase in concentration every half hour, additional frequency shifts were observed in the concentration range 1−100 μg/mL (Figure 7). The binding was highly dependent on the amount of Fab′ bound to the layer. Maximum binding of IgG was attained at the Fab′ fragment concentration 25 μg/mL with a total frequency change of 143 Hz (Figures 6 and 7). The nonspecific binding of BSA at this Fab′ fragment concentration represented approximately 10% of the specific binding. Fab′ fragment concentrations exceeding 25 μg/mL lead to a lower binding of IgG. A layer of Fab′ fragments too tightly packed may prevent IgG from binding to the antibodies because of steric hindrance. As opposed to BSA and human IgG, the bound Fab′ fragments could not be rinsed off the monolayer with a cleaning solution of glycine−HCl at pH = 2.5, a solution often used for

(44) Lohner, K.; Konovalov, O. V.; Samoilenko, I. I.; Myagkov, I. V.; Troitzky, V. I.; Berzina, T. I. *Thin Solid Films* **1996**, *288*, 262.

(45) Ben-Dov, I.; Willner, I.; Zisman, E. *Anal. Chem.* **1997**, *69*, 3506.

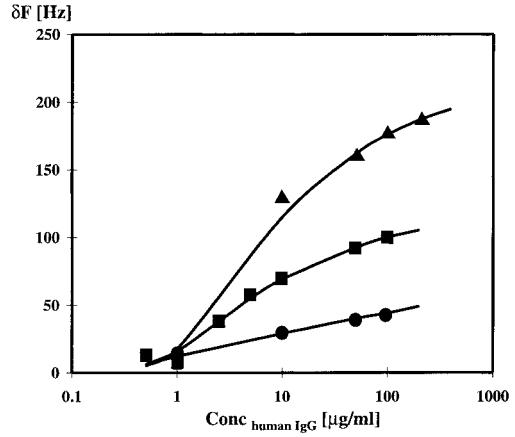

Figure 7. Change in frequency upon binding of increasing concentrations of human IgG to Fab′ fragments bound to a monolayer of DPPC/DPPE-EMCS from 25 μg/mL (▲), 10 μg/mL (■), and 100 μg/mL (●) of Fab′ fragments.

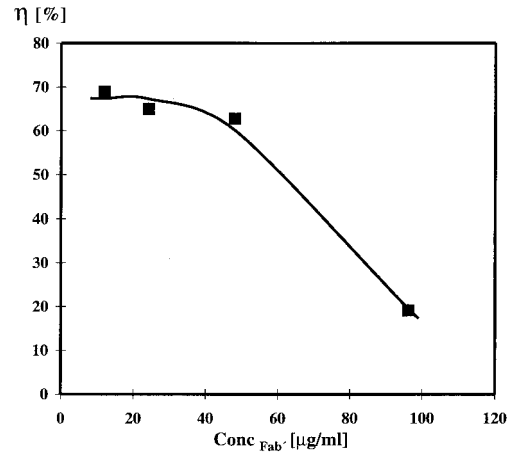

Figure 8. Efficiency of Fab′ fragments attached to a monolayer of DPPC/DPPE-EMCS to bind human IgG.

regeneration of antibody layers. Consequently, the observed decrease in resonant frequency was due to a covalent coupling between EMCS and Fab′ fragments. The maleimidocaproyl group of DPPE-EMCS combines with thiol groups of the Fab′ fragment via an addition reaction to the double bond. The subsequent frequency decrease, on the other hand, can be regarded as a specific affinity interaction between Fab′ fragments coupled to the monolayer and free antigen in the solution. The antibodies, however, lost their IgG binding activity, when treated with the regeneration solution.

The efficiency of the Fab′ fragment to bind human IgG could be calculated from the frequency decrease.[46] The binding efficiency of the Fab′ fragments bound to the DPPC/DPPE-EMCS is shown in Figure 8 as a function of the Fab′ fragment concentration. 67% of the Fab′ fragments bound IgG at low Fab′ fragment concentration. The antigen-binding efficiency decreased with higher Fab′ fragment concentration. The Fab′ fragments might be too closely bound, and steric hindrance may inhibit the immunoreaction, as earlier stated.

Differences in the Operation of the QCM in Air and Liquid. The operation of the QCM in liquid still remains poorly understood. Sauerbreys' equation cannot necessarily be directly applied in the case of direct

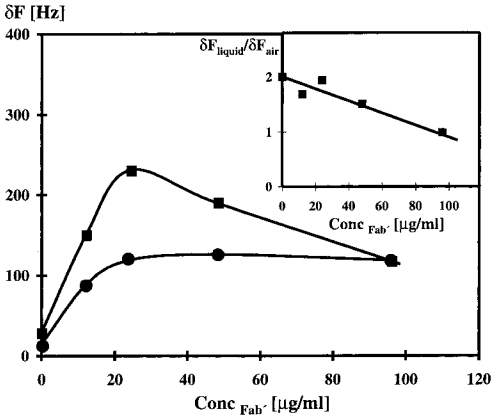

Figure 9. Total change in frequency in liquid (■) and air (●) after binding of Fab′ fragments, 0.1 mg/mL of BSA, and 0.1 mg/mL of human IgG to a monolayer of DPPC/DPPE-EMCS versus Fab′ fragment concentration. The frequency change caused by the lipid monolayer was subtracted from the frequency shift measured in air. The ratio between liquid and air measurements is shown in the inset.

measurements in liquid. The difference between liquid and air measurements seems to be dependent on the protein. Geddes et al.[25] obtained a liquid-to-air ratio of about 2.5 and 3.6 for monolayers of IgG and antibodies, respectively. Even 4-fold frequency changes in liquid versus those in air have been reported.[47] The differences might be due to viscoelastisity changes occurring in the layer, slipping, or entrapped water molecules.[20,48] To evaluate the difference between liquid and air measurements, the total change in frequency after binding of Fab′ fragments, BSA, and human IgG to monolayers of DPPC/DPPE-EMCS was also monitored in air. The mass change of the lipid layer has, however, to be reduced from the responses in air, because the frequency shift caused by the lipid layer was not measured at the liquid−monolayer interface. The QCM response in air attained a saturation value of 88 Hz at a Fab′ fragment concentration of 25 μg/mL, whereas that in liquid had a maximum at this concentration and then decreased (Figure 9). The frequency shift in air corresponded to a Γ of 192 ng·cm^{-2}. The ratio between liquid and air measurements decreased linearly with Fab′ fragment concentration and became close to unity at higher concentrations (Figure 9 inset). The difference could not be due to a poor transfer of the layer or desorption of protein. Almost the same frequency value was achieved if a layer, being rinsed with water and air-dried, was measured in liquid another time. The frequency shift in liquid was probably affected by slippage and/or surface-bound water.[20,47] The coupling of the transversal shear vibrations of the underlying QCM electrode does not distinguish between entrapped water and solid.[47] The ratio between liquid and air measurements was large at low Fab′ fragment concentrations. Thus a larger part of the frequency shift could be due to surface-bound water and/or slippage when low amounts of antibody fragments and human IgG were bound. If the liquid-to-air ratio 1.7 at the Fab′ fragment concentration 25 μg/mL is taken into account, the shift in frequency of 68 Hz caused by the binding of antibody fragments would correspond to a Γ of 87 ng·cm^{-2}. The IgG surface density would, on the other hand, correspond to 184 ng·cm^{-2}. The slippage and/or hydration of the protein layers might,

(46) It was assumed that only 1:1 complexes were formed, and M_r G was taken to be 150 000 for immunoglobulin and 47 000 for the antibody fragment.

(47) Rickert, J.; Brecht, A.; Göpel, W. *Biosens. Bioelectron.* **1997**, *12*, 567.

(48) Albrecht, O.; Gruler, H.; Sackmann, E. *J. Colloid Interface Sci.* **1981**, *79*, 319.

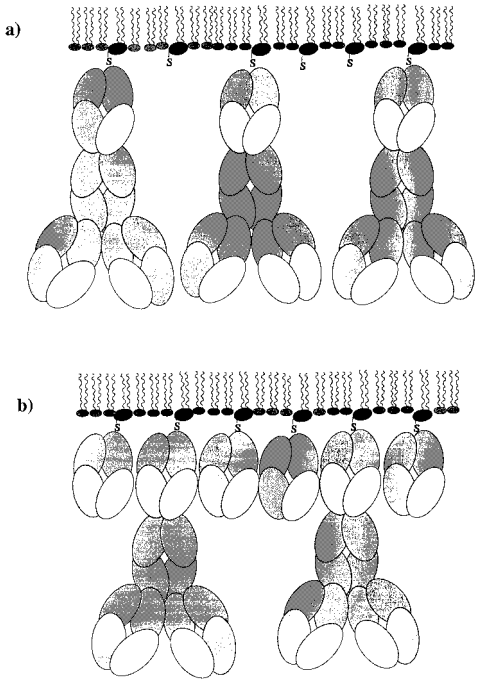

Figure 10. Representations of the attempted configuration of the binding of Fab′ fragments and IgG to a monolayer mixed with linker lipids. Fab′ fragments are bound as about half of a monolayer in part a, whereas the fragments are bound in a closely packed monolayer in part b, causing less IgG to be bound due to steric hindrance.

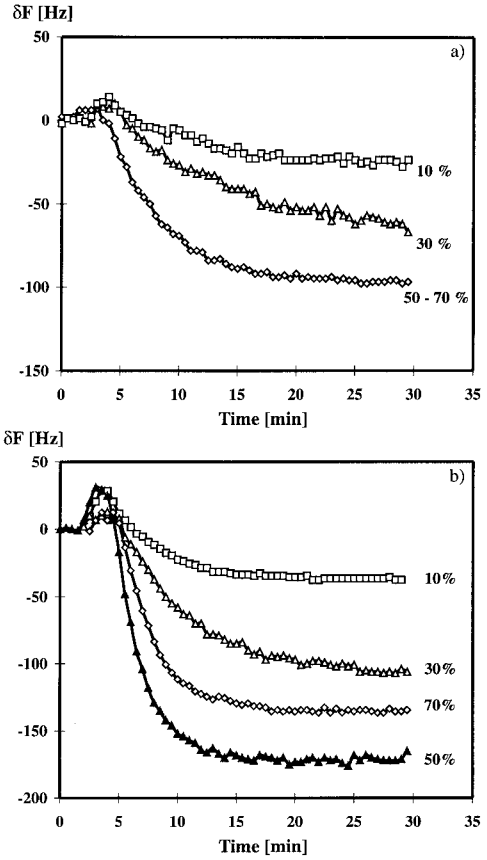

Figure 11. Change in frequency upon (a) binding of Fab′ fragments and (b) the subsequent binding of human IgG to a monolayer of DPPC/DPPE-EMCS/CHOL.

however, not be the same. The scenario for the binding could be the following: when only about half of a monolayer of Fab′ fragments were attached to the linker lipids (Figure 10a), the frequency shift would merely be due to surface-bound water molecules and/or slippage. When the Fab′ fragment concentration increased, the amount of surface-bound water and/or slippage decreased and the frequency shift was dominated by the surface mass of the bound proteins (Figure 10b). The total shift in frequency did not increase above 25 μg/mL of Fab′ fragments, and the ratio between liquid and air measurements became close to unity (Figure 9). The total change in mass of the different configurations in Figure 10 would be the same and thus agree with the air measurements in Figure 9.

Dependence on the Composition of the Monolayer Matrix. Figure 11a shows the change in resonant frequency upon binding of 25 μg/mL of Fab′ fragments onto monolayers of DPPC/DPPE-EMCS/CHOL. Binding equilibrium was obtained within about 10−15 min. The response was dependent on the amount of CHOL in the monolayer matrix. There was a low binding of Fab′ fragments to the layer containing 10 mol % cholesterol. The nonspecific binding of BSA to the layer gave a frequency change of 15 Hz, and the subsequent interaction with IgG was very low (Figure 11b). The monolayer went through a phase transition around 35 mN/m, as seen from the isotherm in Figure 3. DPPC-EMCS was most probably squeezed out of the layer. There would be less amount of linker groups accessible for coupling to the antibody fragment, which would explain the low binding of Fab′ fragments. At a surface pressure of 40 mN/m a mixed phase of DPPC and CHOL coexists with nearly pure DPPC, if the layers contain less than 20% CHOL. A mixed phase of DPPC and CHOL, on the other hand, coexists with nearly pure CHOL above 20% CHOL.[48] An increase in the binding of Fab′ fragments was observed for CHOL concentrations exceeding 10 mol % (Figure 11a). A saturation value of 95 Hz was reached at 50 mol % cholesterol. The highest binding of IgG was observed at this molar ratio. The linker lipids might be differently oriented in the layer compared to the DPPC/DPPE-EMCS layer, because of the condensing effect of cholesterol. The ratio between the shift in frequency in liquid and that in air increased linearly with amount of CHOL in the layer. The amount of water embedded and/or slippage differed from that of the DPPC/DPPE-EMCS matrix. The ratio was about 3.5 for layers containing 50% cholesterol. A total shift in frequency of 290 Hz observed for a layer with 50 mol % CHOL would therefore correspond to 182 ng·cm^{-2} (83 Hz in air). This means that the monolayer would take about the same configuration as Fab′ fragments and human IgG bound to the DPPC/DPPE-EMCS layer. Cholesterol concentrations below and above 50 mol % lead to a lower binding of human IgG. The unspecific binding of BSA to the DPPC/DPPE-EMCS layer was very low but increased slightly with cholesterol in the monolayer matrix (data not shown). Chapman[49] has reported that tightly packed layers of phosphatidylcholine do not readily bind proteins.

The binding efficiency of the Fab′ fragments attached to DPPC/DPPE-EMCS/CHOL layers to interact with IgG was lower than that of those attached to DPPC/DPPE-EMCS (Figure 12). The efficiency of the Fab′ fragments to bind IgG, however, increased with cholesterol content and obtained a maximum binding efficiency of 57% at 50 mol % cholesterol.

Binding of Fab′ Fragments to DPPE-SPDP. Figure 13 shows that the decrease in resonant frequency is very

(49) Chapman, D. *Langmuir* **1993**, *9*, 39.

Table 1. Characteristic Binding Constants and Surface Densities of Anti-Human IgG with Various Immobilization Methods As Measured with RIA and QCM Methods

	RIA				QCM		
monolayer matrix	K_a, $\times 10^9$ M^{-1}	Γ_a, ng·cm^{-2}	Γ_{tot}, ng·cm^{-2}	η_a, %	Γ_a, ng·cm^{-2} %	Γ_{tot}, ng·cm^{-2}	η_a, %
PS/whole antibody	0.24	3.4	111	3.1			
PS/F(ab′)$_2$	0.87	4.8	50	9.6			
DPPC/DPPE-EMCS[a]	0.65	13.8	23.0	60	99	148	67
DPPC/DPPE-EMCS-CHOL[b]	0.78	14.2	58.9	24	118	219	57
DPPC/DPPE-SPDP[c]	0.81	10.2	14.3	71	2	42	4
DPPC/DPPE-SPDP/CHOL[b]	0.34	14.5	66.4	22	31	61	50

[a] DPPC/linker in a molar ratio of 1/9. [b] DPPC/linker/CHOL in a molar ratio of 1/4/5. Fab′ fragments were attached if not otherwise mentioned. Γ_{tot} is the total surface density of the Fab′ immobilized, and Γ_a is the surface density of active Fab′. η_a is the binding efficiency of the antibodies.

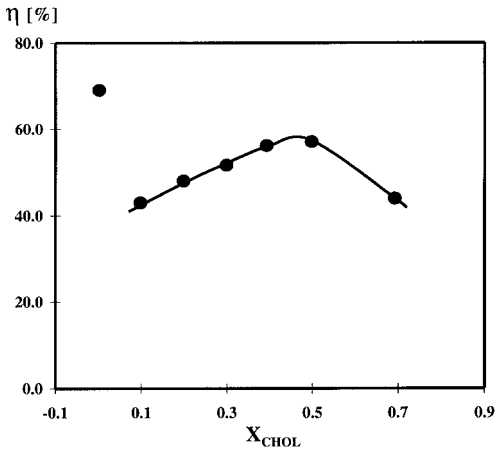

Figure 12. Efficiency of the Fab′ fragments bound to a monolayer of DPPC/DPPE-EMCS/CHOL to bind human IgG.

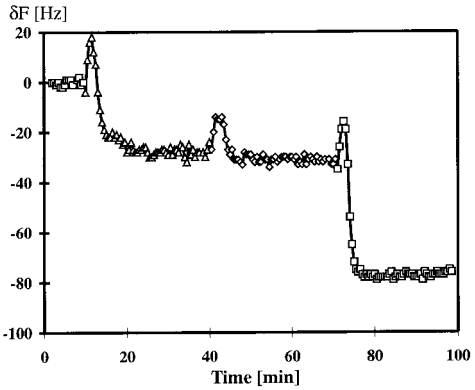

Figure 13. Change in resonant frequency upon binding of 25 μg/mL of Fab′ fragments, 0.1 mg/mL of BSA, and 0.1 mg/mL of IgG to a monolayer of DPPC/DPPE-SPDP/CHOL (4/1/5). The noise of the QCM has increased, because of repeated measurements with the same sensor.

low when Fab′ fragments were pumped into the flow-cell beneath a monolayer of DPPC/DPPE-SPDP/CHOL. The binding of Fab′ fragments to layers containing 50 mol % cholesterol reached a saturation level of 28 Hz within 10 min. An additional frequency decrease of 4 Hz was obtained for the binding of BSA. On the subsequent addition of IgG, a frequency decrease of 46 Hz was observed within 3 min. The efficiency of the Fab′ fragments to bind IgG was still quite high, 50% (Table 1). If cholesterol was not encluded in the layer, the attachment of Fab′ fragments was very low and the binding effeciency for antigen was below 5%. The specific binding of the thiol groups of the Fab′ fragments with the disulfide of DPPE-SPDP[50] was thus poor, if cholesterol was not included in the monolayer matrix. It could be observed from the isotherm, as earlier discussed, that the orientations of DPPE-SPDP and DPPE-EMCS were dissimilar. An unfavorable orientation of DPPE-SPDP might partly explain the low coupling of antibody fragments, but the position of the disulfide might also play a role.

Radioimmunoassay. The amounts of antibody attached to various materials and the specific binding parameters of the immobilized antibody are shown in Table 1. It can be observed that the binding affinity (K_a) is highest for adsorption of F(ab′)$_2$ to polystyrene. The affinity constant for the whole antibody adsorbed to polystyrene was lowest, while the lipid matrices gave values intermediate to these. The immobilization efficiency of the antibodies in terms of recovered binding sites was, however, much higher with the lipid films. The highest recoveries were observed for films without cholesterol (60−70%), while those with cholesterol were already much lower (20−25%), but not so low as for the adsorption to polystyrene (3−10%). Another interesting point to observe was that adsorption of F(ab′)$_2$ to polystyrene gave improved recovery of binding sites and a higher affinity than adsorption of the whole antibody.

The incorporation of CHOL seems to lead to the highest density of specific binding sites but increases the total density of Fab′ relatively more, such that the efficiency drops from the 70% level to the 23% level. A surface density of 47 ng·cm^{-2} has been reported to be attached to maleimide linkers on a plasma-polymerized surface,[16] which is in agreement with our RIA measurements. The total amounts of bound Fab′ fragments and antigen from RIA correlate with those obtained from the QCM measurements, if it is taken into account that the QCM measurements were performed in the aqueous phase, while RIA measurements are based on gravimetric and spectroscopic assessments of the protein concentration, which only reflect the dry weight of the protein. If the liquid-to-air ratio of the QCM measurements is taken into account, the total amounts of Fab′ fragments attached to the DPPE-EMCS layers with and without cholesterol as measured with RIA are only a factor of 2 lower than those obtained from QCM. The RIA measurements differ by a factor of 0.4 for DPPC/DPPE-SPDP/CHOL but agree for DPPC/DPPE-SPDP. It is, however, considerable that the binding efficiency of Fab′ fragments attached to the DPPC/DPPE-SPDP layer at the monolayer−air interface was much lower than that of the transferred layers. Transfer of the layers onto the silicon slides most probably affects the binding of Fab′s to the linker groups. The transfer ratios of the layers, furthermore, vary. The transfer ratio could not be measured exactly because of the small size of the slides, but it was noticed that layers with CHOL were better transferred.

(50) Smyth, D. G.; Nagamatsu, A.; Fruton, J. S. *J. Am. Chem Soc.* **1960**, *86*, 1839.

Conclusions

These studies show that it is possible to control the density and orientation of antibodies by attaching them covalently to linker lipids in a monolayer matrix. The orientation of the coupled Fab′ fragments is critically dependent on matrix composition, as demonstrated here for EMCS versus SPDP. Nonspecific binding levels depend also critically on the monolayer matrix. The overall highest density of specific binding sites was obtained by including cholesterol in the monolayer matrix, which may be utilized in immunosensor technology. The highest overall binding efficiency, however, was obtained for monolayers without cholesterol, reaching 70% activity of the monolayer. The latter monolayer matrix may thus be useful for highly efficient immunoassays that additionally require a minimum amount of Fab′.

An important observation was that the QCM detection gave on average a much larger surface density than the radiotracer method, a feature that can be explained by hydration and/or slippage in the protein layer that are additionally detected by the QCM device.

Further studies will deal with transfer of the lipid layer to a novel type of flow-cell. The in situ measurements with the QCM resonator will be continued, and the sensitivity and detection limit of the device will be assessed. We also study presently the regeneration of the Fab′ layer, as well as its stability for prolonged use. There is also work in progress on coupling of Fab′ fragments via different types of spacers between the lipid and the Fab′. Polymerizable linker lipids are also going to be used to further increase the stability of the Fab′ layer.[51,52]

Acknowledgment. The authors would like to thank H. Helle and H. Välimäki for technical assistance with the QCM. This work was supported by the Academy of Finland and the Technical Research Centre of Finland.

LA971412X

(51) Watson, H.; Peltonen, J. *Sens. Actuators* **1997**, *38*−*39*, 261.
(52) Viitala, T.; Peltonen, J.; Albers, M.; Vikholm, I. *Langmuir*, accepted.